Lattice-stiffening transition in gadolinium chains on furrowed (112) surfaces

2004 J. Phys.: Condens. Matter 16 4711

(http://iopscience.iop.org/0953-8984/16/26/006)

INSTITUTE OF PHYSICS PUBLISHING JOURNAL OF PHYSICS: CONDENSED MATTER

J. Phys.: Condens. Matter **16** (2004) 4711–4724 PII: S0953-8984(04)76339-0

Lattice-stiffening transition in gadolinium chains on furrowed (112) surfaces

Ya B Losovyj[1,2], I N Yakovkin[3], Hae-Kyung Jeong[2], David Wisbey[2] and P A Dowben[2,4]

[1] Department of Physics and Astronomy and Center for Materials Research and Analysis, University of Nebraska, Lincoln, NE 68588-0111, USA
[2] Center for Advanced Microstructures and Devices of Louisiana State University, 6980 Jefferson Highway, Baton Rouge, LA 70806, USA
[3] Institute of Physics of National Academy of Sciences of Ukraine, Prospect Nauki 46, Kiev 03028, Ukraine

E-mail: pdowben@unl.edu

Received 18 February 2004
Published 18 June 2004
Online at stacks.iop.org/JPhysCM/16/4711
doi:10.1088/0953-8984/16/26/006

Abstract

A lattice-stiffening transition is observed near 230 K in corrugated 'chain like' gadolinium structures formed on Mo(112) and W(112). This transition is evident from the change in the effective Debye temperature. Below the transition temperature of 230 K the gadolinium overlayer lattice has much higher effective Debye temperature than that observed for higher temperatures (for the quasi-one-dimensional Gd sub-monolayer structures or for the higher coverage overlayers). From model studies, lateral dipole–dipole and indirect interactions as well as the interaction between the adatoms and the substrate play an important role in this transition.

1. Introduction

Lattice distortions, including both longitudinal distortions (a Peierls distortion) and transverse distortions (a transverse Peierls distortion) have been predicted to occur for quasi-one-dimensional overlayers structures [1, 2]. These structural distortions should be accompanied by profound changes in the electron phonon coupling [2]. Distortions, in generalized one-dimensional models, can also involve spins (magnetic polarons) and charge (lattice polarons), with the consequence that there should be an increase in compressibility [3]. This type of lattice stiffening transition has been observed for a crystal made of oriented and parallel insulating polymer chains, with large intramolecular dipoles [4].

[4] Author to whom any correspondence should be addressed.

Quasi-one-dimensional chain-like structures are commonly observed on corrugated or 'furrowed' substrate surfaces like the (112) surfaces of Mo and W [1, 2] and include adlayers of large moment 4f metals like gadolinium. The widely separated chains of gadolinium in the 1×7 structure on W(112) (figures 1(c), (d)) suggest an electronic interaction between the chains mediated by the W(112) surface electronic structure [1, 5], so these systems cannot, by any stretch of the imagination, be considered 'pure' one-dimensional systems. Yet, the presence of a more localized band structure characteristic of gadolinium and large moments [6] does provide further opportunities for identifying more examples of a compressibility transition [3] distinguished by a dramatic change (with temperature) in the experimentally derived effective Debye temperatures. In this paper, a lattice-stiffening transition in Gd chain structures on Mo(112) and W(112) will be discussed as a function of temperature and Gd coverage ($\theta = n_{\mathrm{Gd}}/n_{\mathrm{W}}$). The lattice-stiffening transition has been found for gadolinium adlayers on both substrates, and appears to be associated with the formation of chain-like overlayer structures.

2. Experiment

Low energy electron diffraction (LEED), scanning tunnelling microscopy (STM), x-ray photoemission spectroscopy (XPS) and angle-resolved photoemission experiments were undertaken in separate UHV chambers with a base pressure of 1×10^{-10} Torr. The surface topography was obtained using VT Omicron STM in the constant current mode. The angle-resolved photoemission spectra were obtained using a photon energy of 16 eV in combination with a hemispherical electron energy analyser with photoelectrons collected normal to the surface, as described elsewhere [7, 8]. With the highly plane-polarized synchrotron light, photoemission experiments were undertaken with polarization varied from p-polarization (65° off normal), with the vector potential oriented more normal than parallel to the surface, to s + p polarization (40°–45° measured from normal) with the photoelectrons collected along surface normal. The XPS studies were completed with a Gammadata Scienta SES-100 electron energy hemispherical analyser and a SPECS x-ray source.

Two furrowed substrates, Mo(112) and W(112), were used to grow adlayers of gadolinium at submonolayer and multilayer coverages. These substrates have very similar properties such as lattice constant and structure, but different band widths [9]. The substrate surfaces were prepared using standard methods of flashing and annealing in oxygen [7, 10]. The W(112) and Mo(112) sample substrate was oriented with respect to the crystallographic plane (112) with accuracy of about 20 arcmin. Gadolinium was deposited under 1×10^{-10} Torr with minimum degassing by thermal heating. Figures 1(a)–(f) show LEED and schematic structures of clean W(112) with increasing gadolinium coverages. The electron energies used in low electron diffraction LEED were between 50 and 70 eV in order to minimize the electron mean free path.

3. The chain structures

On many surfaces, notably the refractory metal surfaces of tungsten and molybdenum, the gadolinium overlayer adopts a sequence of ordered structures with increasing coverage, and grows, at least initially, layer by layer [7, 10, 11]. Defining coverage here by $\vartheta = n_{\mathrm{Gd}}/n_{\mathrm{W}}$ (the ratio of the surface concentration of the Gd adatoms n_{Gd} and surface W(112) atoms n_{W}), as the coverage of Gd increases on W(112), the adlayer chain-like p(1×7) structure and c(2×2) structure form at the coverages of 0.14 and 0.5 respectively, after mild annealing (500 K). The low energy electron diffraction pattern and corresponding schematic structures,

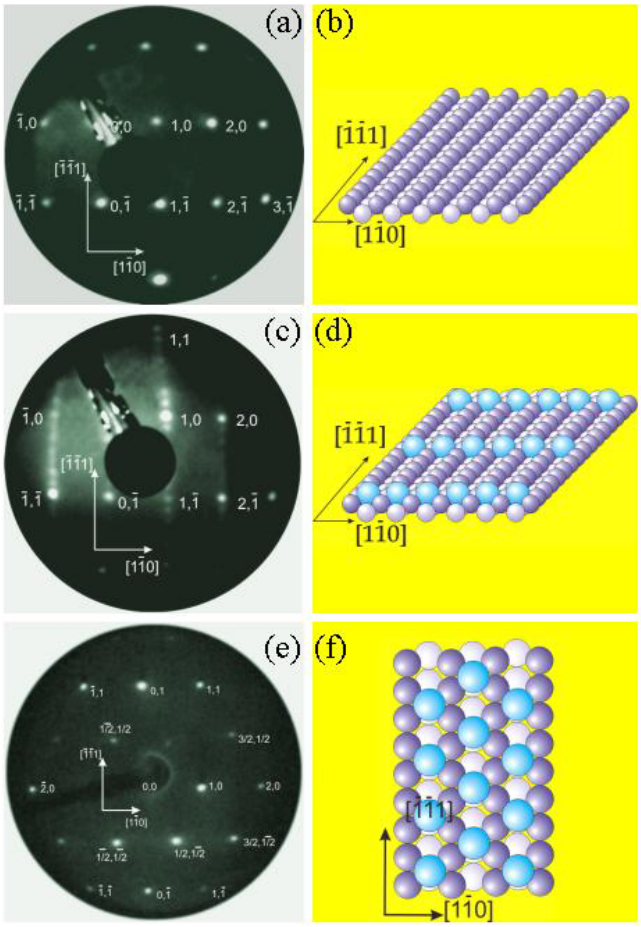

Figure 1. Clean W(112) ((a), (b)), Gd p(1 × 7) ((c), (d)) and Gd c(2 × 2) structures formed on W(112) ((e), (f)) are illustrated. Both LEED patterns ((a), (c), (e)) and schematic structures ((b), (d), (f)) are shown.

for both the linear chain p(1 × 7) structure (figures 1(c), (d)) and the closer packed c(2 × 2) structure (figures 1(e), (f)) submonolayer commensurate structure of gadolinium on W(112), are presented in figure 1. The complete gadolinium monolayer on W(112) forms at a coverage of $\vartheta = 0.78$. Gd overlayers, at a coverage of slightly more than 1 ML on the Mo(112) substrate, also form a chain structure (STM inset to figure 3) which corresponds to a p(16 × 6) commensurate structure on the Mo(112) substrate ($\vartheta = 1.04$–1.15).

4. Changing Debye temperature

While the true surface Debye temperature, containing the in-plane and anharmonic motions, is difficult to measure in most surface spectroscopies [12], the effective surface Debye temperature can be readily obtained using LEED, XPS, EELS (electron energy loss spectroscopy), IPES (inverse photoemission spectroscopy) and other surface sensitive techniques [12–22]. The experimentally derived effective surface Debye temperature from

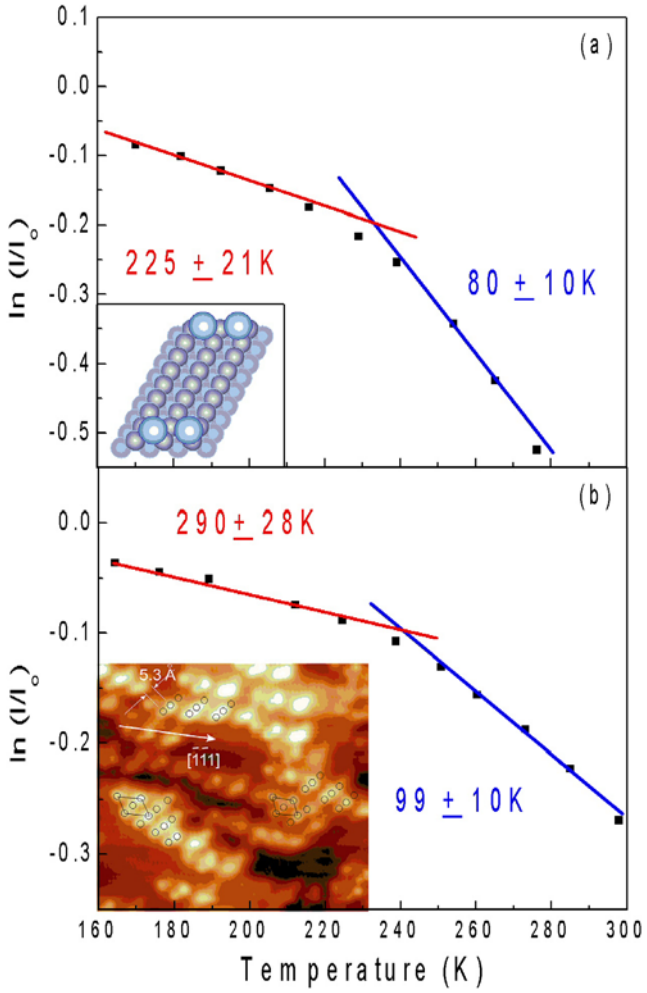

Figure 2. Natural logarithm of integrated intensities from a 'fractional order' Gd induced LEED beam, as a function of temperature, are shown for two coverages corresponding to the p(1 × 7) (a) and c(2×2) (b) Gd structures on W(112). The data for $\vartheta = 0.14$ (a) are accompanied by a schematic of the pertinent p(1 × 7) structure shown as an inset, and for $\vartheta = 0.5$ (b) the corresponding STM image for the c(2 × 2) structure is shown as an inset.

such efforts is mostly a signature of the dynamic motion of vibrational modes normal (transverse or perpendicular to the chain) to the surface [12].

Since the intensity of an emitted or scattered electron beam exponentially decays with increasing temperature, due to increases in the thermal vibration, we can calculate the Debye temperature with careful analysis of the intensity change as a function of temperature:

$$I = I_0 \exp(-2W)$$
$$2W = \frac{3\hbar^2 T(\Delta k)^2}{2mk_B\Theta_D^2} \tag{1}$$

where W is the Debye–Waller factor, T is the temperature of the sample (in kelvin), $\hbar(\Delta k)$ is the electron momentum transfer, m is the mass of the scattering centre, k_B is the Boltzmann constant and Θ_D is the Debye temperature. Because of the different scattering geometries,

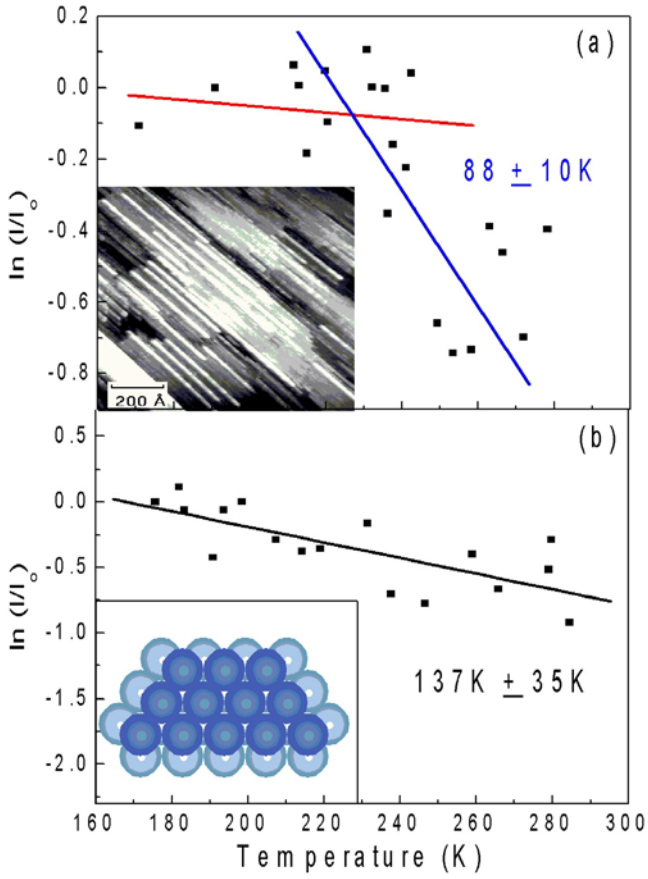

Figure 3. Natural logarithm of integrated intensities from the Gd 4f peak, obtained from x-ray photoemission spectra, as a function of temperature, are shown for two coverages of gadolinium films on Mo(112). For the 4 Å thick gadolinium film on Mo(112) (a), the data are shown with the corresponding STM image, in the inset, which shows quasi-one-dimensional Gd chains. For the 19 Å thick gadolinium film on Mo(112) (b), the adlayer structure adopts that of a hexagonal surface as schematically shown in the inset.

we estimate the electron momentum transfer differently for XPS and LEED. For LEED, the momentum transfer is

$$|\Delta\vec{k}| = |\vec{k}_{\mathrm{f}} - \vec{k}_{\mathrm{i}}| = \left|2k\cos\frac{\theta}{2}\right| \tag{2}$$

where θ is the angle between surface normal and diffracted electron beam. The mass of a Gd atom is the mass of the scattering centre. Due to the geometry of LEED, θ is very small and $\sin^2\frac{\theta}{2}$ (parallel component) is much smaller than $\cos^2\frac{\theta}{2}$ (normal component).

For low energy electron diffraction, the fractional order scattered low energy beams, near specular, but characteristic of the overlayer structure, were used to extract the intensity with temperature $I(T)$ to minimize substrate contributions. (The substrate integral order beams were used to obtain the substrate Debye temperatures for reference.) Largely from these data we extracted the effective Debye temperature, but comparisons with x-ray photoemission show similar trends.

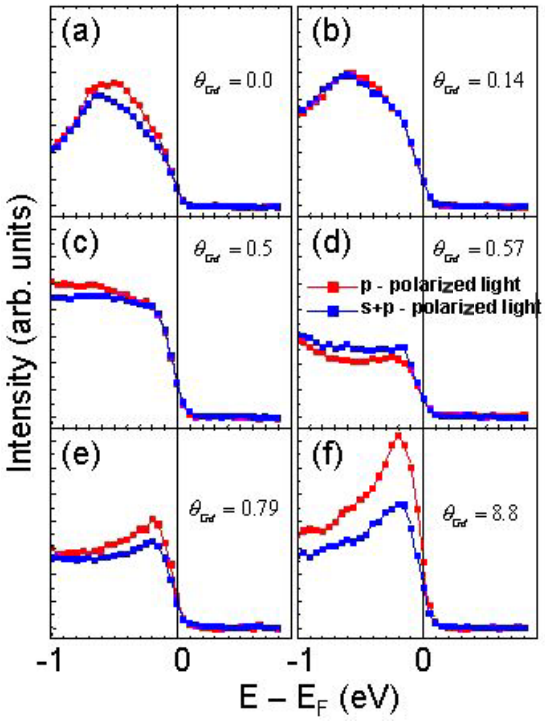

Figure 4. Normal photoemission spectra of Gd on W(112) obtained with p- and s + p-polarized light. The spectra obtained with s + p-polarized light are denoted by blue symbols and the spectra from p-polarized incident radiation by red symbols. Gd coverages are 0, 0.14, 0.5, 0.57, 0.79 and 8.8 for panels (a)–(f), respectively.

For XPS, the momentum transfer is the momentum of the emitted photoelectron. Since the electron analyser was used to collect the photoelectrons normal to the surface, the motion normal to the surface is again the dominant contribution to the Debye–Waller factor. In XPS, the element of origin for the emitted photoelectron determines the mass of the scattering centre [12, 14, 15].

The integrated intensity of the diffracted electron beam from LEED, as a function of temperature, shows a dramatic reduction in intensity above about 230 K for both the p(1 × 7) and c(2 × 2) structures on W(112), as seen in figure 2. There are two basic reasons why this dramatic drop in LEED scattering intensity can occur: either there is a structural phase transition or a change in the electron–phonon coupling. There is no evidence in scanning tunnelling microscopy, nor any indication in LEED, of a structural transition. Phonon effects are therefore implicated. Major phonon effects lead to deviations in the behaviour expected from equation one, as is observed here.

Using the above analysis of the scattering intensity, we have determined that the Debye temperature, for the p(1 × 7) structure ($\vartheta = 0.14$) on W(112) is 225 ± 21 K below 220 K but 80 ± 10 K above 240 K, as seen in figure 2(a). As the gadolinium coverage on W(112) increases to 0.5 (the c(2 × 2) structure, $\vartheta = 0.5$), similar behaviour in the Debye temperature is observed with an experimentally extracted effective Debye temperature of 290 ± 28 K occurring below about 230 K and 99 ± 10 K above about 250 K, derived from the LEED intensities as shown in figure 1(b).

The integrated intensities of x-ray photoemission spectra show similar behaviour for Gd on Mo(112). As shown in figure 3(a) for Gd of 4 Å thickness on Mo(112), the experimentally determined Debye temperature is 88 ± 10 K above about 230 K. Below 230 K, we have not been able to extract the effective Debye temperature, but clearly the value is much higher. Evidently the same sort of transition (between two vastly different effective Debye temperatures) occurs with the chain like structures on both W(112) and Mo(112).

This change in the effective Debye temperature, with temperature, for submonolayer coverages of gadolinium on W(112) must be associated with the gadolinium adlayer. The accepted Debye temperature of tungsten is about 310 K [21, 22]. No similar behaviour is observed for W(112). Upon completion of the gadolinium monolayer, the experimentally extracted Debye temperature is 245 ± 10 K, and slowly decreases to 140 ± 35 K with increasing gadolinium coverage. Similarly, the change in Debye temperature observed with the lower coverage gadolinium structure on Mo(112) must be due to the gadolinium overlayer. The Mo(112) effective surface and bulk Debye temperatures are 313 and 422 K, respectively [12]. For thicker Gd overlayer films (19 Å) on Mo(112) the phase transition disappears and the Debye temperature is 137 ± 35 K (figure 3(b)), in agreement with the values determined from heat capacity (119 K) [23] and the elastic constants (128 K) [24, 25].

The change in effective Debye temperature, with temperature, indicates that a lattice-stiffness transition occurs at near 230 K. Below the transition temperature of 230 K the gadolinium overlayer lattice has greater stiffness than at higher temperatures. The lattice-stiffness phase transition happens for both commensurate submonolayer structures W(112) and for the chain like structures formed by gadolinium at slightly more than a monolayer on Mo(112). Since in LEED no obvious adlayer structural distortion is observed to occur across the transition temperature, the obvious explanation of a Peierls distortion [1, 2] cannot be easily invoked.

5. The intra-chain bonding and strong substrate interactions

There is an evolution of the density of states near the Fermi edge region with increasing coverages of Gd from the submonolayer to multilayer coverages, and the states near the Fermi level exhibit a change in band symmetry with increasing gadolinium coverage on W(112). Up to a coverage of $\vartheta \leqslant 0.5$, the surface resonance state of W(112) at 0.4 eV binding energy [9] is only slightly perturbed, with an additional density of states appearing at about 0.2 eV binding energy. Above the coverage of $\vartheta = 0.5$, the tungsten substrate surface states are strongly suppressed and only the contribution to the density of states in the vicinity of 0.2 eV binding energy is seen to increase with increasing coverage. The addition of gadolinium to the surface, up to a coverage of $\vartheta \leqslant 0.5$, results in a weak contribution to the W(112) surface resonance band intensities at 0.4 eV, as shown in figure 4, as well as to the W(112) surface resonance band intensities at 1.5 eV, and bulk band intensities at about 3 eV binding energy. At increasing coverages thereafter, additional gadolinium contributes to bands at about 2.3 eV binding energy and 0.2 eV binding energy. The fact that several W(112) bands are perturbed at gadolinium coverages less than $\vartheta \leqslant 0.5$ suggests that the gadolinium atoms in the submonolayer coverage range are hybridized with the W(112) surface electronic structure as the $5d^1 6s^2$ configuration of gadolinium cannot support two or more fully occupied bands unless spin is considered.

The widely separated chains of gadolinium in the 1×7 structure on W(112) suggest an electronic interaction between the chains mediated by the W(112) surface electronic structure [1, 5]. Indirect interaction between adsorbed atoms on a metal surface [5, 26–32] relates intimately to the oscillations in electron density when screening an impurity in the volume of a metal [33–36]. The energy of the indirect interaction oscillates with distance, while

the period is determined by the Fermi vector k_F. Thus the formation of the gadolinium p(1 × 7) linear structure on the W(112) not only confirms strong hybridization between the gadolinium and the substrate but also indicates the minimum in potential of the indirect interaction between the chains at a distance of 7 periods of the substrate along the furrows.

The gadolinium coverage regimes of $\vartheta \leqslant 0.5$, $0.5 \leqslant \vartheta < 0.79$ and $\vartheta > 0.79$ on W(112), are characterized by distinct changes in symmetry. Since the light from the synchrotron is highly plane-polarized, from a comparison of light incidence angle photoemission spectra corresponding symmetry assignments for photoelectrons collected along the surface normal can be made. For $\theta = 45°$, the incident light is a combination of s-polarized, and p-polarized light while at $\theta = 70°$, the light is strongly p-polarized. Since, at $\overline{\Gamma}$, the point group symmetry is C_{2v} the bands observed in photoemission must be a_1 (s, p_z, $d_{3z^2-r^2}$), b_1 (p_x, d_{xz}) or b_2 (p_y, d_{yz}).

At coverages up to the completion of the c(2 × 2) structure on W(112), from the decreased enhancement of this band in p-polarized light, it is evident that the symmetry a_1 ($d_{3z^2-r^2}$ and s) character of the 0.4 eV binding energy W(112) surface state is lost or destroyed while the density of states is not suppressed. This again is consistent with strong hybridization between the electrons of the gadolinium adatom with the W(112) substrate electrons.

The development of a new peak at about of 0.2 eV binding energy at gadolinium coverages in the range of $0.5 \leqslant \vartheta < 0.79$, on W(112), is accompanied by an enhancement of this peak in s + p-polarized light. This is clearly seen already at $\vartheta = 0.57$ (figure 4(d)). Thus in this coverage range, there is the development of interface states (or gadolinium states, that still must contain contributions from the W(112) substrate). The enhancement of intensity is characteristic of $d_{xz}d_{yz}$ character, not the a_1 ($d_{3z^2-r^2}$ and s) symmetry character observed at higher coverages.

We have found that the intensity at 0.2 eV binding energy increases with increasing coverage for $\vartheta > 0.5$, up to 10 monolayers on W(112). For coverages $\vartheta \geqslant 0.79$, or a little above one monolayer, the gadolinium state is also increasingly pronounced in p-polarized light. This enhancement of this state in p-polarized light is characteristic of the a_1 ($d_{3z^2-r^2}$ and s) symmetry character observed for the gadolinium surface state on many different substrates [1–5]. It is only with coverages above a monolayer that a gadolinium band of a_1 symmetry ($d_{3z^2-r^2}$ and s symmetry character) is observed. It is only above a monolayer that two chemically different gadolinium species are present in the adlayer on W(112). There is no surprise that the gadolinium coverage must be more than a monolayer of gadolinium for the surface state of gadolinium to become established. The surprise is that the surface state is established so quickly at coverages above a monolayer.

With increasing gadolinium coverage, the general trend is that the effective Debye temperature of the gadolinium adlayer first increases from about 225 to about 290 K, then slowly falls with increasing gadolinium coverage. What is unusual is that at temperatures of about 230 to 250 K, the gadolinium chain like structures exhibit a drop in the experimentally determined Debye temperature. These phase transition temperatures are near the effective Debye temperature characteristic of normal motion. Since these low coverage structures on W(112) are characterized by band symmetries $d_{xz}d_{yz}$ character, near the Fermi level, not shared by clean tungsten or higher coverages of gadolinium, the band symmetries of these frontier orbitals may play a role in this lattice stiffening phase transition.

Although we do not have direct evidence, once the surface normal vibrational modes are excited, occurring at about the effective Debye temperature of 250–290 K for the chain like gadolinium structures, dynamic displacements in the chain will occur. These transverse displacements both along the surface normal and along the furrows of these corrugated substrate surfaces may not be static, but it is easily conceivable that the in plane gadolinium–gadolinium bonds of $d_{xz}d_{yz}$ character will weaken far faster, in spite of strong interactions with the substrate,

than bonding through bands of $a_1(d_{3z^2-r^2}$ and s) symmetry character. We speculate that this transition does resemble a transverse 'inverse' Peierls distortion (occurring with increasing rather than decreasing temperature), but since we do not observe evidence of a structural distortion in LEED, we suggest that these distortions are dynamic rather than static, i.e. there are position fluctuations of the atoms in the chain, weakening the chain, but not changing the overall 'average' structure. Different electron–phonon coupling parameters are expected with changes with band symmetry.

6. The stability of the gadolinium chains

We can model the lattice stiffening transition (and higher temperature chain 'melting' transition at about 400 K) of these gadolinium chains by exploiting the observed structural periodicity [7, 10, 11] and our knowledge of the substrate band structure [9]. Formation of the linear structures originates from competition between lateral repulsion of the dipoles μ (that are polarized adatoms with their images) and substrate-mediated indirect interaction [5, 26–32]. Such a separation of lateral interactions into a dipole–dipole term $2\mu^2/r^3$, and oscillatory term $A\cos(2k_Fr)/r^n$, implies that the latter corresponds to the indirect exchange interaction [37, 38] rather than just electrostatic, while the oscillations of the potential with interatomic distance r originate from Friedel oscillations [39] with the period dictated by Fermi vector k_F.

Lau and Kohn [32] showed that screening in a two-dimensional electron gas provides a long-range behaviour of the potential, with r^{-2} asymptotic. Hence, surface states and resonances at a metal surface can accomplish a long-range oscillatory interaction between adatoms. Recently, this form of effective potential and the r^{-2} asymptotic of indirect interaction have been further justified in experiment [40] and by Monte Carlo simulations of formation of CO structures on Pt(111) surface [41]. A one-dimensional screening [42–44] results in a r^{-1} asymptotic of lateral interaction, which could significantly contribute to the formation of long-period structures. This one-dimensional model has been exploited for a qualitative explanation of results of LEED studies of structures and phase diagrams for Li overlayers and Sr overlayers Mo(112) [44–48].

The quasi one-dimensional screening in the direction along surface atomic rows, due to the anisotropic geometry of the W(112) surface, is illustrated in figure 5. Assuming both dipole–dipole and indirect interaction are responsible for formation of the structures of adsorbed gadolinium films, the effective potential of lateral interaction can be roughly estimated as

$$V(r) = \frac{2\mu^2}{1.6r^3} + A\cos(2k_Fr + \phi)\begin{cases} r^{-1} \text{ along rows} \\ r^{-2} \text{ elsewhere} \end{cases} \tag{3}$$

(with the dipole moment μ in Debye, the 1.6 factor in the denominator provides values of the potential in eV). The r^{-1} asymptotic behaviour of the indirect interaction is assumed to originate from quasi one-dimensional electron states in atomic rows of the W(112) surface, while the r^{-2} form, adopted for other directions at the surface, follows from behaviour that is characteristic for a two-dimensional screening at the surface [32].

The potential of lateral interaction is defined by the dipole moment μ (for Gd on W(112), at low coverages, μ is roughly 1.8 D), the amplitude A, Fermi wavevector k_F, and the phase ϕ (which can be taken to be zero, in keeping with spirit of the linear theory of one-dimensional screening [32, 37, 43]). The k_F can be ascribed to the crossing point for surface resonance bands along the $\overline{\Gamma}$–$\overline{X}$ direction in the surface Brillouin zone (that is, along the furrows), which has been determined for W(112) as $k_F = 0.4$ Å^{-1} both in the angle-resolved photoemission experiments and theory [9]. With this value, the effective potential of lateral interaction along the rows reveals a pronounced minimum at $7a_1$ (figure 5), essential for formation of the p(1 × 7)

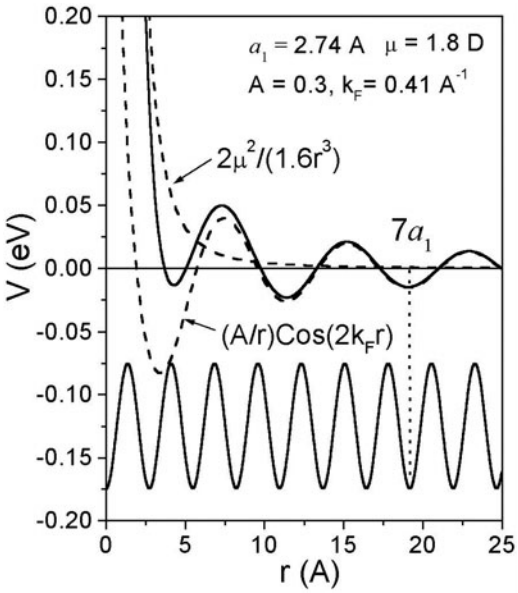

Figure 5. Effective potential of lateral interaction between Gd adatoms along atomic rows of the W(112) surface. Potentials of the dipole–dipole and indirect interactions are shown by dashed curves.

structure of Gd films on the W(112) surface. The lateral interaction along the Gd chains could also be attributed to the competition between electrostatic repulsion and indirect interaction, but, because of small distances between the adatoms and probable inverse cubic power of such interactions, such an empirical decomposition does not seem very applicable.

The energy of the effective lateral interaction in the Gd chains is described by the parameter ε_0, which, as well as the amplitude A, can be estimated from our Monte Carlo simulations from the best fit between experimental and simulated low energy electron diffraction intensities with temperature $I(T)$ curves in the range of the order–disorder transition at near 400 K. As indicated in figure 6, the LEED patterns characteristic of the p(1×7) and c(2×2) structures are lost at extremely elevated temperatures, which we take to be characteristic of chain melting. In fitting this high temperature LEED intensity data, for Gd films on W(112), with simulated overlayers with great disorder undertaken as discussed below, the amplitude of the indirect interaction and energy of interaction between Gd adatoms in the chains, derived from the best fit to the experimental $I(T)$ plots, are $A = 0.3$ eV Å and $\varepsilon_0 = -30 \pm 5$ meV.

The simulations were performed using the Metropolis algorithm, which is a well-recognized technique for Monte Carlo modelling of the formation of structures in the two-dimensional lattice gas model, and is appropriate for commensurate adsorbed layers [49–51]. The surface is represented by a rectangular matrix which contains 0 when the corresponding site is vacant, or 1 when occupied. The size of the matrix should be sufficient to obtain reasonable statistics, and usually the adopted area is about the coherence width of typical low energy electronic diffraction experiments $\sim$100 Å $\times$ 100 Å. Periodic boundary conditions are introduced to simulate an infinite surface. It should be noted also that the number of rows and columns in the matrix must be taken with respect to the expected film structure to prevent formation of artificial domain walls at the boundaries. Thus, for simulation of the p(1×7) structure, 'smooth' boundary conditions are satisfied with 42 rows. Obviously, the adopted

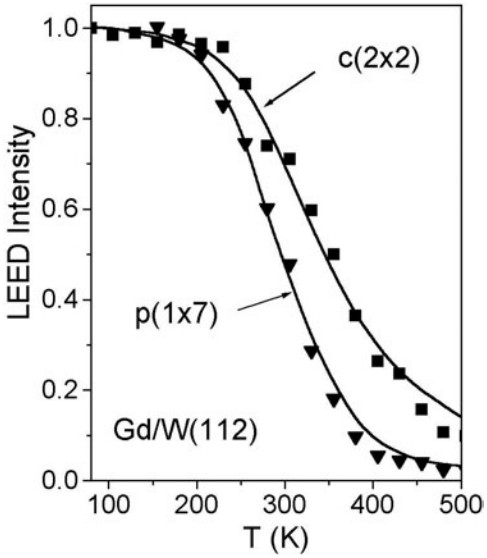

Figure 6. Intensity of the LEED beams for the p(1 × 7) and c(2 × 2) structures of Gd on the W(112) surface as a function of temperature. Experimental data are shown by solid curves while symbols denote Monte Carlo results.

description of lateral interaction requires an accounting for interactions between Gd atoms for rather large separations. In our simulations, the radius of effective interaction was chosen to be of $10a_1$, that is, interactions between a given atom and all atoms within this region were calculated explicitly (using equation (3)).

The first step is the deposition of a certain number of particles into randomly chosen sites to obtain the desirable coverage. Then, a randomly chosen particle can move to a vacant neighbouring site (along surface furrows only, because the difference of diffusion coefficients for directions along and across the furrows of Mo(112) is three orders in magnitude [49]). The probability W of the move depends on gain in energy, ΔE. If the energy of lateral interaction increases due to the move, $\Delta E > 0$, then, according to Boltzmann statistics, $W = \exp(-\Delta E/k_{\mathrm{B}}T)$. If the move leads to a decrease of the energy, then $W = 1$. As a result of many such moves, the free energy approaches minimum for a given temperature [30, 50–52]. Hence, when the temperature is below the transition point, an ordered structure is formed, while at higher temperatures the film is disordered.

Relative intensities of LEED reflections can be estimated within the kinematical approximation [48, 50, 51] as

$$I(h,k) = \left| \sum_n \exp\{2\pi(hx_n + ky_n)\} \right|^2 \tag{4}$$

which yields a model LEED pattern [43]. The summation here is performed over occupied sites with the x_n and y_n coordinates defined in terms of fractions of the 'cell', which can be taken as the part of the surface under consideration, while the h and k denote reciprocal space coordinates. By taking arbitrary h and k, it is possible to simulate the distribution of LEED intensities over the screen, thus following transformations of the patterns with ordering the film structures [30, 41]. To mimic the diffraction patterns, the LEED beams are depicted by circles whose sizes indicate the intensity, as evaluated according to equation (4). The comparison of the experimental low energy electron diffraction intensities versus $I(T)$ for the gadolinium p(1 × 7)

and c(2×2), with the Monte Carlo simulations, are shown in figure 6, and agreement is excellent across both the transition at 240 K, as well as when the chains 'melt' in the region of 400 K.

There are two important conclusions following from a good agreement between the Monte Carlo simulations and the experimental LEED intensities:

(i) The lattice gas model provides a reasonable description of the order–disorder (chain melting) transition. This feature implies the equivalence of adsorption sites for the Gd atoms in the 1×7 chains and in the c(2×2) structure.
(ii) The first order phase transition between the p(1×7) and c(2×2) structures indicates the importance of attraction between the Gd adatoms in the c(2×2) structure, which becomes stronger than the attraction in the linear chains when the dipole–dipole repulsion decreases due to depolarization of adsorbed Gd atoms.

Recall that formation of both structures has been obtained with the same value of ε_0, that is effective interaction along the chains, while an attractive potential for the c(2×2) structure originates from the indirect interaction along atomic rows of the W(112) surface. Hence, on increasing coverage, there is no substantial change in the nature of lateral interaction, but the indirect interaction can be accomplished by different groups of electrons at the Fermi surface. In particular, it may be expected that these indirect 'bonds' will be of different symmetry for the p(1×7) and c(2×2) gadolinium structures. This is certainly consistent with the change in observed band symmetry in the gadolinium state near the Fermi energy at $\vartheta \geqslant 0.5$, as noted in the previous section.

Other large period two-dimensional rare earth structures, mediated by substrate density of state have been observed [53]. The large separations between Ce atoms in the 32 Å superlattice formed on Ag(111) are mediated indirect interactions involving the Ag(111) surface state band, similar to the mechanism for the order of the gadolinium chains on W(112) reported here. For this large period superlattice of Ce on Ag(100), a potential well of 4.9 ± 0.5 meV and a trapping barrier height of 11.8 ± 1.2 meV was experimentally determined [53].

7. Conclusions

In conclusion, we have found the lattice-stiffening transition near 240 K in Gd submonolayers on W(112) and in the chain like structures formed on Mo(112). This phase transition is unique to lower coverage gadolinium structures, on the W(112) or Mo(112) substrates, and is not evident in thicker gadolinium films with an $a_1(d_{3z^2-r^2}$ and s) character surface state near the Fermi level. The behaviour of the lattice stiffening transition is very similar to that observed in insulating polymer chains [4].

The use of a lateral interaction dipole–dipole term of the form $2\mu^2/r^3$, in our model calculations, with pronounced dipoles oriented along the surface normal is very similar to the insulating polymer chains [4] where intramolecular dipole–dipole interactions are quite pronounced, but are weak between the chains [54, 55]. Given the similarities between the lattice stiffening transition observed here and that previously reported for polymer chains, we propose that a significant dipole–dipole coupling interaction term within the chain is key. An anomalous lattice stiffening transition has also been previously reported for $La_{2-x}Sr_xCuO_4$ across the superconducting transition [56], and as with other high temperature superconductors, this lattice stiffening is associated with strain in the lattice but no direct comparison can be made with the lattice stiffening transition seen here.

The amplitude of the indirect interaction and energy of interaction between Gd adatoms in the chains, derived from the best fit to the experimental $I(T)$ plots, are $A = 0.3$ eV Å and $\varepsilon_0 = -30 \pm 5$ meV.

Acknowledgments

The support of the NSF 'QSPINS' MRSEC (DMR 0213808), W M Keck Foundation Center for Mesospin and Quantum Information Systems, the Center for Materials Research and Analysis (CMRA), and the Nebraska Research Initiative at the University of Nebraska are gratefully acknowledged.

References

[1] Yakovkin I N 2001 *J. Nanosci. Nanotechnol.* **1** 357–74
[2] Dowben P A 2000 *Surf. Sci. Rep.* **40** 151–247
[3] Moreo A, Yunoki S and Dagotto E 1999 *Science* **283** 2034
[4] Borca C N, Adenwalla S, Choi J, Sprunger P T, Ducharme S, Robertson L, Palto S P, Liu J, Poulsen M, Fridkin V M, You H and Dowben P A 1999 *Phys. Rev. Lett.* **83** 4562–5
[5] Braun O M and Medvedev V K 1989 *Sov. Phys.—Usp.* **32** 328
[6] Yakovkin I N, Komesu T and Dowben P A 2002 *Phys. Rev.* B **66** 035406
[7] Waldfried C, McIlroy D N and Dowben P A 1997 *J. Phys.: Condens. Matter* **9** 10615
[8] Li D, Hutchings C W, Dowben P A, Wu R-T, Hwang C, Onellion M, Andrews A B and Erskine J L 1991 *J. Appl. Phys.* **70** 6565
[9] Losovyj Ya B, Yakovkin I N, Jeong H-K and Dowben P A 2004 *Phys. Status Solidi* **241** 829
[10] Gonchar F M, Medvedev V K, Smereka T P, Losovyj Ya B and Babkin G V 1987 *Sov. Phys.—Solid State* **29** 1629
[11] Weller D and Alvarado S F 1986 *J. Appl. Phys.* **59** 2908–13
[12] Waldfried C, McIlroy D N, Zhang J, Dowben P A, Katrich G A and Plummer E W 1996 *Surf. Sci.* **363** 296–302
[13] Jeong H-K, Komesu T, Dowben P A, Schultz B D and Palmstrøm C J 2002 *Phys. Lett.* A **302** 217–23
[14] Van Hove M A, Weinberg W H and Chan C M 1986 *Low-Energy Electron Diffraction* (*Springer Series in Surface Science* vol 6) (Berlin: Springer) p 134
[15] Clarke L J 1985 *Surface Crystallography* (New York: Wiley)
[16] Borca C N, Ristoiu D, Komesu T, Jeong H-K, Hordequin Ch, Pierre J, Nozieres J P and Dowben P A 2000 *Appl. Phys. Lett.* **77** 88–90
[17] Borca C N, Xu B, Komesu T, Jeong H K, Liu M T, Liou S H and Dowben P A 2002 *Sci. Lett.* **512** L346
[18] Tonner B P, Li H, Robrecht M J, Chou Y C, Onellion M and Erskine J L 1986 *Phys. Rev.* B **34** 4386
[19] Williams R S, Wehner P S, Stöhr J and Shirley D A 1977 *Phys. Rev. Lett.* **39** 302
[20] Kevan S D and Shirley D A 1980 *Phys. Rev.* B **22** 542
[21] Clarke L J and Morales de la Garza L 1980 *Surf. Sci.* **99** 419
[22] Debe J K, King D A and Marsch F S 1977 *Surf. Sci.* **68** 437
[23] Wells P, Lanchester P C, Jones D W and Jordan R G 1974 *J. Phys. F: Met. Phys.* **4** 1729–35
[24] Rosen M 1968 *Phys. Rev.* **174** 504
[25] Palmer S B, Lee E W and Islam M N 1974 *Proc. R. Soc.* A **338** 3411
[26] Einstein T L 1978 *CRC Crit. Rev. Solid State Mater. Sci.* **7** 261
[27] Grimley T B 1967 *Proc. Phys. Soc.* **90** 751
[28] Grimley T B 1967 *Proc. Phys. Soc.* **92** 776
[29] Grimley T B 1968 *J. Am. Soc.* **90** 3016
[30] Kuppers J 1971 *Vacuum* **21** 393
[31] Tsong T T 1972 *Phys. Rev.* B **6** 417
[32] Lau K H and Kohn W 1978 *Surf. Sci.* **75** 69
[33] Friedel J 1952 *Phil. Mag.* **43** 153
[34] Gabovich A M, Il'chenko L G, Pashitskiy E A and Romanov Yu A 1978 *JETP* **75** 249
[35] Melechko A V, Braun J, Weitering H H and Plummer E W 1999 *Phys. Rev. Lett.* **83** 999
[36] Weitering H H, Melesko A, Carpinelli J M, Zhang J, Bartkowiak M and Plummer E W 1999 *Science* **285** 2107–10
[37] Ruderman M A and Kittel C 1954 *Phys. Rev.* **96** 99
[38] Kasuya T 1956 *Prog. Theor. Phys.* **16** 45
Yosida K 1957 *Phys. Rev.* **106** 893
[39] Friedel J 1958 *Nuovo Cimento* **7** (Suppl.) 287
[40] Knorr M, Brune H, Epple M, Hirstein A, Schneider M A and Kern K 2002 *Phys. Rev.* B **65** 115420 see [12]
[41] Petrova N V and Yakovkin I N 2002 *Surf. Sci.* **519** 105

[42] Gabovich A M and Pashitskii E A 1976 *Sov. Phys.—Solid State* **18** 220
[43] Gumhalter B and Brenig W 1995 *Surf. Sci.* **336** 326
[44] Oleksy Cz and Lorenc J 1996 *Phys. Rev.* B **54** 5955
[45] Kolthoff D and Pfnur H 2000 *Surf. Sci.* **459** 265
[46] Fedorus A, Godzik G, Koval V, Naumovets A and Pfnur H 2000 *Surf. Sci.* **460** 229
[47] Fedorus A, Kolthoff D, Koval V, Lyuksyutov I, Naumovets A and Pfnur H 2000 *Phys. Rev.* B **62** 2852
[48] Oleksy Cz 2003 *Surf. Sci.* **543** 5
[49] Naumovets A G, Paliy M V, Vedula Yu S, Loburets A T and Senenko N B 1995 *Prog. Surf. Sci.* **48** 59
[50] Tsong T T 1982 *Surf. Sci.* **122** 99
[51] Medvedev V K and Yakovkin I N 1979 *Sov. Phys.—Solid State* **21** 187
[52] Yakovkin I N 1993 *Surf. Sci.* **282** 195
[53] Silly F, Pivetta M, Ternes M, Patthey F, Pelz J P and Schneider W-D 2004 *Phys. Rev. Lett.* **92** 016101
[54] Choi J, Tang S-J, Sprunger P T, Dowben P A, Fridkin V M, Sorokin A V, Palto S P, Petukhova N and Yudin S G 2000 *J. Phys.: Condens. Matter* **12** 4735–45
[55] Duan C-G, Mei W N, Yin W-G, Liu J, Hardy J R, Ducharme S and Dowben P A 2004 Simulations of ferroelectric polymer film polarization: the role of dipole interactions *Phys. Rev.* B submitted
[56] Nohara M, Suzuki T, Maeno Y, Fujita T, Tanaka I and Kojima H 1995 *Phys. Rev.* B **52** 570